Macromolecules
ARTICLE

Macromolecules **2010**, *43*, 4679–4687 **4679**
DOI: 10.1021/ma100535h

Effects of Supercritical CO_2 Conditioning on Cross-Linked Polyimide Membranes

Adam M. Kratochvil and William J. Koros*

School of Chemical & Biomolecular Engineering, Georgia Institute of Technology, Atlanta, Georgia 30332-0100

Received March 9, 2010; Revised Manuscript Received April 16, 2010

ABSTRACT: The effects of supercritical CO_2 ($scCO_2$) conditioning on high-performance cross-linked polyimide membranes is examined through gas permeation and sorption experiments. Under supercritical conditions, the cross-linked polymers do not exhibit a structural reorganization of the polymer matrix that was observed in the non-cross-linkable, free acid polymer. Pure gas permeation isotherms and mixed gas permeabilities and selectivities show the cross-linked polymers to be much more stable to $scCO_2$ conditioning than the free acid polymer. In fact, following $scCO_2$ conditioning, the mixed gas CO_2 permeabilities of the cross-linked polymers increased while the CO_2/CH_4 separation factors remained relatively unchanged. This response highlights the stability and high performance of these cross-linked membranes in aggressive environments. In addition, this response reveals the potential for the preconditioning of cross-linked polymer membranes to enhance productivity without sacrificing efficiency in practical applications which, in effect, provides another tool to "tune" membrane properties for a given separation. Finally, the dual mode model accurately describes the sorption and dilation characteristics of the cross-linked polymers. The changes in the dual mode sorption model parameters before and after the $scCO_2$ exposure also provide insights into the alterations in the different glassy samples due to the cross-linking and $scCO_2$ exposure.

1. Introduction

Supercritical carbon dioxide ($scCO_2$) continues to be studied for many different applications across a variety of industries. The attractiveness of $scCO_2$ lies in its tunable solvating power and its environmentally favored properties over traditional organic solvents. The use of $scCO_2$ for essential oil and lipid extractions continues to be explored due to the low viscosity and high diffusivity of $scCO_2$ and its protection against thermal degradation since the supercritical temperature of CO_2 is so low. Another attractive feature of using $scCO_2$ for these extractions is the lack of any residual solvent with the product.[1−4] $scCO_2$ also continues to be studied as a solvent in polymerization reactions, especially when its use can eliminate the need for harmful additives such as fluorinated surfactants.[5,6] Another field where $scCO_2$ is proving useful is tool and equipment decontamination of radioactive metal salts and oxides at nuclear power facilities.[7] Inherent in all of these processes though is the high cost of compression to reuse CO_2 when it is depressurized to separate the CO_2 from the solute. Membrane separations provide a means of capturing the desired solute with minimized recompression costs.

In addition, because of environmental concerns of increased CO_2 in the atmosphere, CO_2 sequestration is becoming a viable alternative to simply releasing it into the atmosphere. To make better use of the high-pressure CO_2, enhanced oil recovery and enhanced coalbed methane (ECBM) recovery through the injection of $scCO_2$ are currently being studied.[8−10] $scCO_2$ is preferred over N_2 in ECBM recovery due to its higher solubility in coal which allows for increased methane production and longer breakthrough times.[10] Under constant pressure $scCO_2$ injection, once breakthrough occurs, though, the partial pressure of CO_2 will continue to increase until production stops. Therefore, a backend separation process is required to purify the produced methane and recapture the CO_2. The high pressures and concentrations of CO_2 associated with ECBM recovery favor membrane separations over traditional natural gas separation techniques.

Inorganic membranes are immune to the swelling effects of CO_2, known as plasticization, that are present in glassy polymers and typically degrade the separating efficiency of the membrane. However, inorganic membranes tend to be too difficult to mass produce on a large scale and are often too brittle for use in real-world applications. In order to make use of glassy polymer membranes, which are easily manufactured on a large scale through solution processing, for CO_2 separations, significant research efforts have been conducted to covalently cross-link the polymer. Such cross-linking provides enhanced plasticization resistance and can also provide intrinsic selectivity increases in some cases.[11−13] In addition, Kosuri and Koros exploited the strong hydrogen-bonding nature of a polyamide−imide. The added intersegmental attraction in such materials behaves somewhat like cross-linking and allows manufactured asymmetric hollow fiber membranes that withstood the plasticizing environment of $scCO_2$.[14] Permeabilities tend to be lower in the polyamide−imide family, however, due to the higher cohesive energy density of the hydrogen-bonded matrix.

In our previous study of $scCO_2$ conditioning of high-performance glassy polymers, a surprising result of a structural reorganization of the polymer matrix was discovered.[15] Counter to plasticization which increases membrane permeability, under $scCO_2$ conditions this structural reorganization resulted in significantly reduced membrane permeability and hence productivity. Therefore, the work in this paper was conducted to study the effects of covalent cross-linking on the stability of a high-performance glassy polymer under $scCO_2$ conditioning. As with the previous study, the cross-linked membranes are conditioned with $scCO_2$ and probed with a 50/50 CO_2/CH_4 feed mixture to determine how conditioning affects the membrane performance.

*Corresponding author. E-mail: William.Koros@chbe.gatech.edu.

Published on Web 04/22/2010

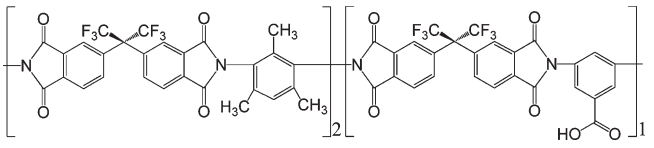

Figure 1. Structure of 6FDA-DAM:DABA (2:1).

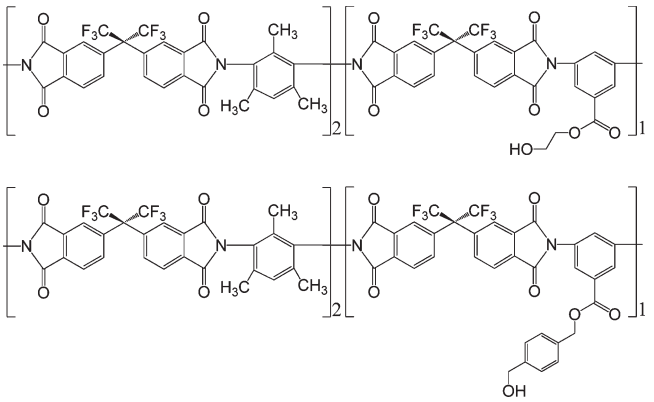

Figure 2. Structures of the ethylene glycol and 1,4-benzenedimethanol monoesterified 6FDA-DAM:DABA (2:1) polymer.

These results have direct application to the ECBM recovery discussed above and can be fundamentally applied to the other applications which can make use of membrane separations for a $scCO_2$ process.

2. Materials and Methods

2.1. Polymer Preparation and Cross-Linking. The structure of the base polyimide, referred to as the "free acid", due to the available carboxylic acid, used in this work is shown in Figure 1. The free acid polymer was synthesized through a polycondensation reaction between the dianhydride and corresponding diamines. The resulting polymer was then precipitated, washed, ground up, and dried. Further details of this synthesis procedure are described in our earlier publication. The free carboxylic acid group enables subsequent cross-linking through a condensation reaction involving diol cross-linking agents. The cross-linking agents chosen for this work are ethylene glycol and 1,4-benzenedimethanol. These cross-linking agents represent the smallest possible cross-link and a large, rigid cross-link in order to better understand the effects of cross-linking under $scCO_2$ conditions.

To create a cross-linkable polymer, ~5−10 g of the free acid polymer was added to NMP to make a 6 wt % solution. An acid catalyst, *p*-toluenesulfonic acid, was then added in the amount of 1.7 mg catalyst/g polymer, and a large excess of glycol was added in the amount of ~70 times the stoichiometric requirement. This solution was then heated to 140 °C for 18−24 h to react one end of the glycol to the carboxylic acid and form the monoesterified polymer. The structures of these monoesterified polymers are shown in Figure 2. During this heated step, water was distilled from the solution to drive the reaction toward esterification.[16] The monoesterified polymer solution was then precipitated in the same way as the polymer synthesis. Dense films of the free acid and monoesterified polymers were formed by casting a 3−5% weight solution in THF into a Teflon dish in an inert environment. Subsequent heat treatment of the films at 220 °C for 48 h completed the cross-linking reaction in the monoesterified polymers and provided a similar thermal history for the free acid films as the cross-linked films. Further details of this cross-linking procedure are described elsewhere.[17]

2.2. Gas Permeation. Gas permeation measurements were conducted in a constant volume-variable pressure system. The $scCO_2$ conditioning permeation isotherms were conducted at 35 °C and consist of a pressurization cycle up to 1500 psia at 150 psi intervals, ~10 days at constant pressure, and a depressurization cycle at 150 psi intervals. Because of the plasticizing nature of CO_2, true steady-state permeabilities cannot be obtained since glassy polymers have a tendency to undergo long-term drifts that can persist for several days. Even though the rate of these drifts is pressure dependent, these changes in permeability over time are relatively small compared to the absolute permeability values. Therefore, a defined time interval of 12 h was chosen for each pressure stage following which the permeability measurement was taken in order to rationally compare the major effects of cross-linking to the un-cross-linked free acid membrane. After the measurement, the pressure was immediately increased to the next interval set point. Following the 10 day isobaric conditioning, the depressurization cycle was started. This cycle consisted of a 5 h pressure reduction at a rate of 0.5 psi/min and a 7 h conditioning time at that pressure interval, following which the permeability measurement was taken. The protocol for the repressurization cycle was identical to the pressurization cycle. The mixed gas permeation measurements were collected after 10 time lags of the slow gas and analyzed by gas chromatography. Further details of the mixed gas measurements can be found in the earlier publication.[15] While characterizing the detailed long-term drifts in such complex glasses is interesting, it is not the primary focus of the present work.

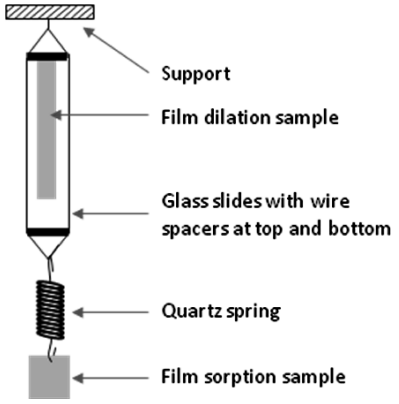

Figure 3. Dilation and sorption sample holder for Jerguson gauge.

2.3. Sorption and Dilatometry. Measurement of sorption and volumetric dilation of the glassy polymers studied here was conducted using a modified high-pressure Jerguson transparent gauge. The dilation sample was sandwiched between two glass slides and fixed at the upper end to allow measurements of the free-standing lower end as the polymer dilates. Metal wires were attached into place at the top and bottom of one of the glass slides to maintain a gap of about 160 μm between the slides while allowing free expansion of the 25−40 μm thick film samples. The quartz spring was attached to a wire hook at the bottom of the glass slides to allow the sorption sample to be suspended beneath the dilation sample. A schematic of the dilation and sorption sample holders is shown in Figure 3. Two cathetometers were then set to measure the movements of both samples during experiments. The buoyancy of the polymer sample, the copper wire holding the sample, and the spring were corrected for in the sorption calculations. The sorption and dilation conditioning cycles were identical to the permeation pressurization and depressurization cycles along with a ten day isobaric conditioning period at 1500 psia. An Isco syringe pump was used to pressurize the CO_2 into the supercritical state for conditioning measurements.

2.4. Fluorescence Spectroscopy. Charge transfer complexes are coplanar overlaps between π-bonding orbitals in the aromatic groups of the polymer. Such complexes are known to form in polyimides through the alignment of electron-donating and

electron-accepting portions of the backbone.[18−20] Fluorescence spectroscopy was used to characterize the extent of charge transfer complexing in the cross-linked polyimides in this work. Polymer films were measured using a 50× objective at 365 nm on a CRAIC 1000 spectrometer.

3. Results and Discussion

3.1. Gas Permeation Experiments. *3.1.1. Pure Gas.* Our prior work revealed the effects of $scCO_2$ conditioning on the free acid polymer through the structural reorganization observed in the permeability isotherm. This isotherm of the free acid polymer is shown again in Figure 4 for reference. Figure 5 presents the CO_2 permeability isotherms for both cross-linked polymers. The clear difference between these isotherms and the free acid isotherm, in Figure 4, is the lack of the observed structural reorganization at high pressures in the cross-linked polymers. In the earlier work, it was shown that low sorbing gases, He and N_2, do not induce any permeability collapse in a related polyimide (6FDA-DAM) even though this polymer showed the same permeability collapse as seen in the un-cross-linked free acid for of the (6FDA-DAM-DABA), so it appears likely that the strong sorption tendency of CO_2 is the key factor enabling it to induce the permeability collapse reported for the un-cross-linked free acid. In any case, the ability of the cross-linking to prevent this permeability collapse is quite interesting. Upon depressurization, the cross-linked polymers exhibit a hysteretical response that is typical of glassy polymers. While the larger benzenedimethanol cross-linking agent was expected to prop open the polymer structure and enhance permeability, the CO_2 permeabilities are actually similar to those of the ethylene glycol at lower pressures. Moreover, at higher pressures, the CO_2 permeabilities in the 1,4-benzenedimethanol cross-linked polymer actually remain lower than that of the ethylene glycol cross-linked polymer. As mentioned in the prior publication, fugacity-based permeabilities are nearly identical to these pressure-based permeabilities. Fluorescence spectra were obtained for the two cross-linked polymers to determine if the aromatic nature of the 1,4-benzenedimethanol

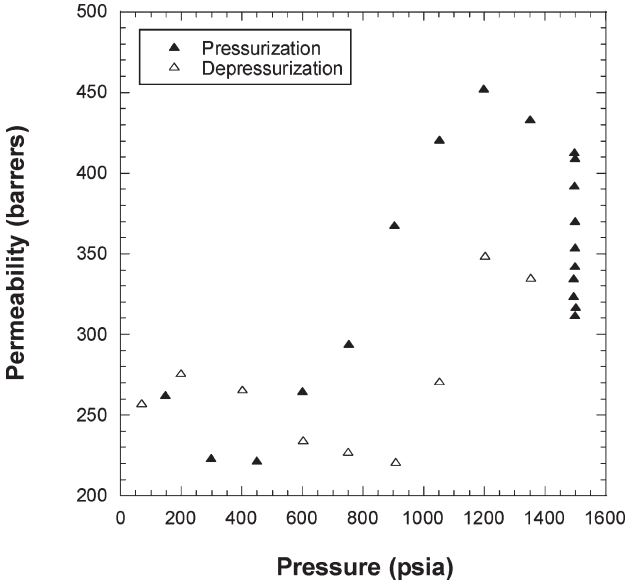

Figure 4. CO_2 permeability isotherm for 6FDA-DAM:DABA (2:1) free acid polymer displaying the structural reorganization under $scCO_2$ conditions.

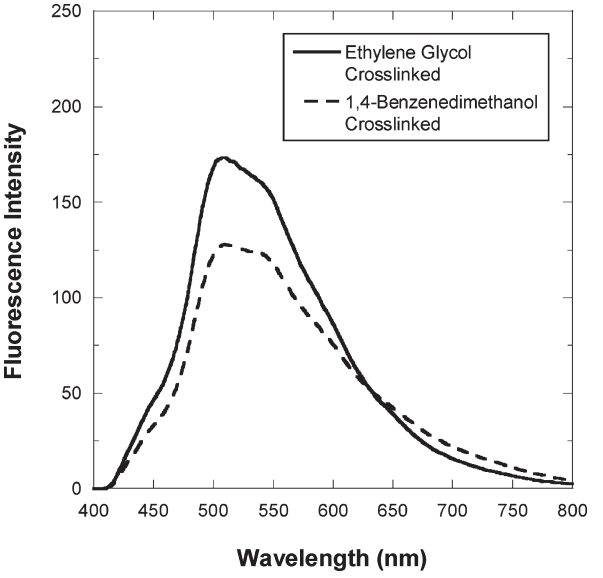

Figure 6. Fluorescence spectra of the cross-linked polymers.

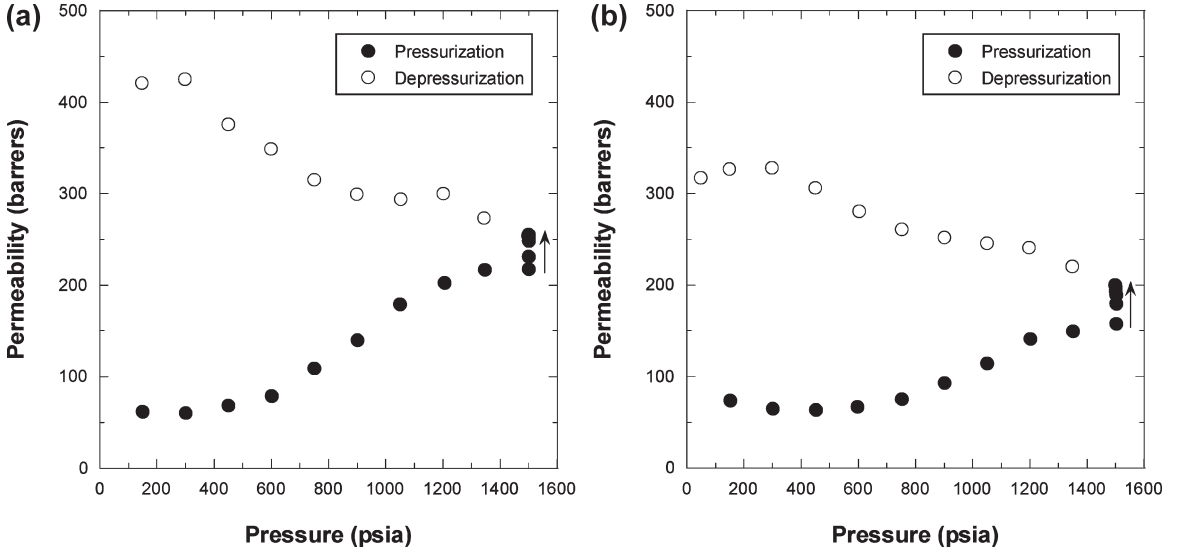

Figure 5. CO_2 permeability isotherms for the (a) ethylene glycol cross-linked and (b) 1,4-benzenedimethanol cross-linked polymers.

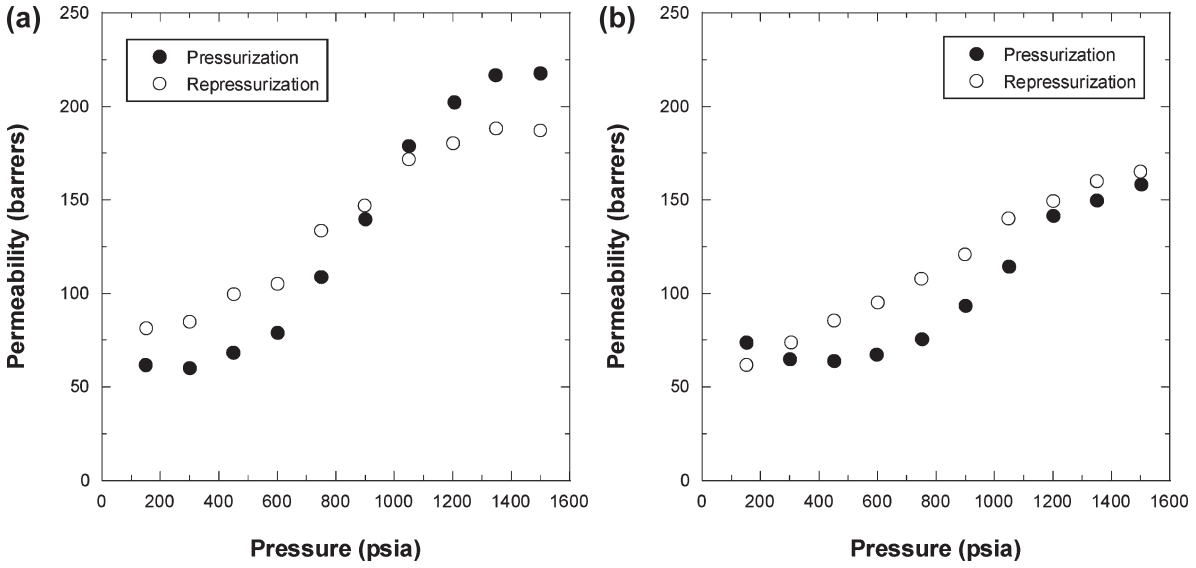

Figure 7. CO_2 permeability isotherms of the (a) ethylene glycol cross-linked and (b) 1,4-benzenedimethanol cross-linked polymers for the pressurization and repressurization cycles.

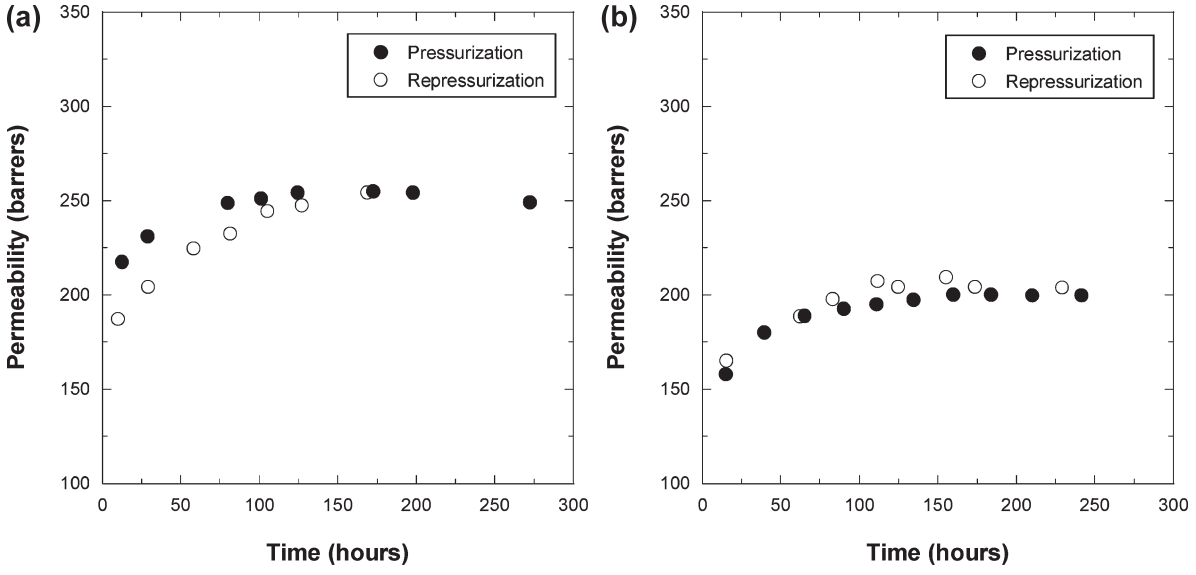

Figure 8. CO_2 permeability of the (a) ethylene glycol cross-linked and (b) 1,4-benzenedimethanol cross-linked polymers as a function of time at 1500 psia.

cross-linking agent might contribute to the formation of charge transfer complexes, which would facilitate a reduction in polymer chain mobility and gas permeability. As shown in Figure 6, the 1,4-benzenedimethanol cross-linked polymer exhibits a lower fluorescence intensity than the ethylene glycol cross-linked polymer, indicating the stiff cross-linking agent actually inhibits the formation of charge transfer complexes. Therefore, the reduced CO_2 permeabilities at high CO_2 pressures in the 1,4-benzenedimethanol cross-linked film is solely a result of the cross-linking agent size and rigidity and not of any interactions the cross-linking agent may have with the polymer backbone. Ultimately, the 1,4-benzenedimethanol cross-linked film is more stabilized in the $scCO_2$ environment, as revealed by the lower CO_2 permeability at 1500 psia, and returns to a lower free volume state upon depressurization as compared to the ethylene glycol cross-linked film.

The repressurization permeation isotherms for both cross-linked films are presented in Figure 7. Again, the 1,4-benzenedimethanol cross-linked film exhibits greater stability than the ethylene glycol cross-linked film upon repressurization as shown by the lower CO_2 permeability at 1500 psia. Neither film exhibits the large decline in CO_2 permeability at the onset of repressurization indicative of structural reorganization as observed in the free acid polymer; however, both cross-linked films have reduced plasticization pressures, indicating that some level of the structural reorganization has occurred. Surprisingly, $scCO_2$ conditioning on the ethylene glycol cross-linked film during repressurization has a less substantial effect than during pressurization which is evident by the lower CO_2 permeability at 1500 psia. Conversely, the 1,4-benzenedimethanol cross-linked film exhibits an expected response for a cross-linked stabilized film in that the CO_2 permeability at higher pressures during repressurization is similar to that during pressurization.

Even though the ethylene glycol cross-linked film appears to be more stabilized during repressurization, the film returns to the same equilibrium state when conditioned at 1500 psia. This response is presented in Figure 8 where the

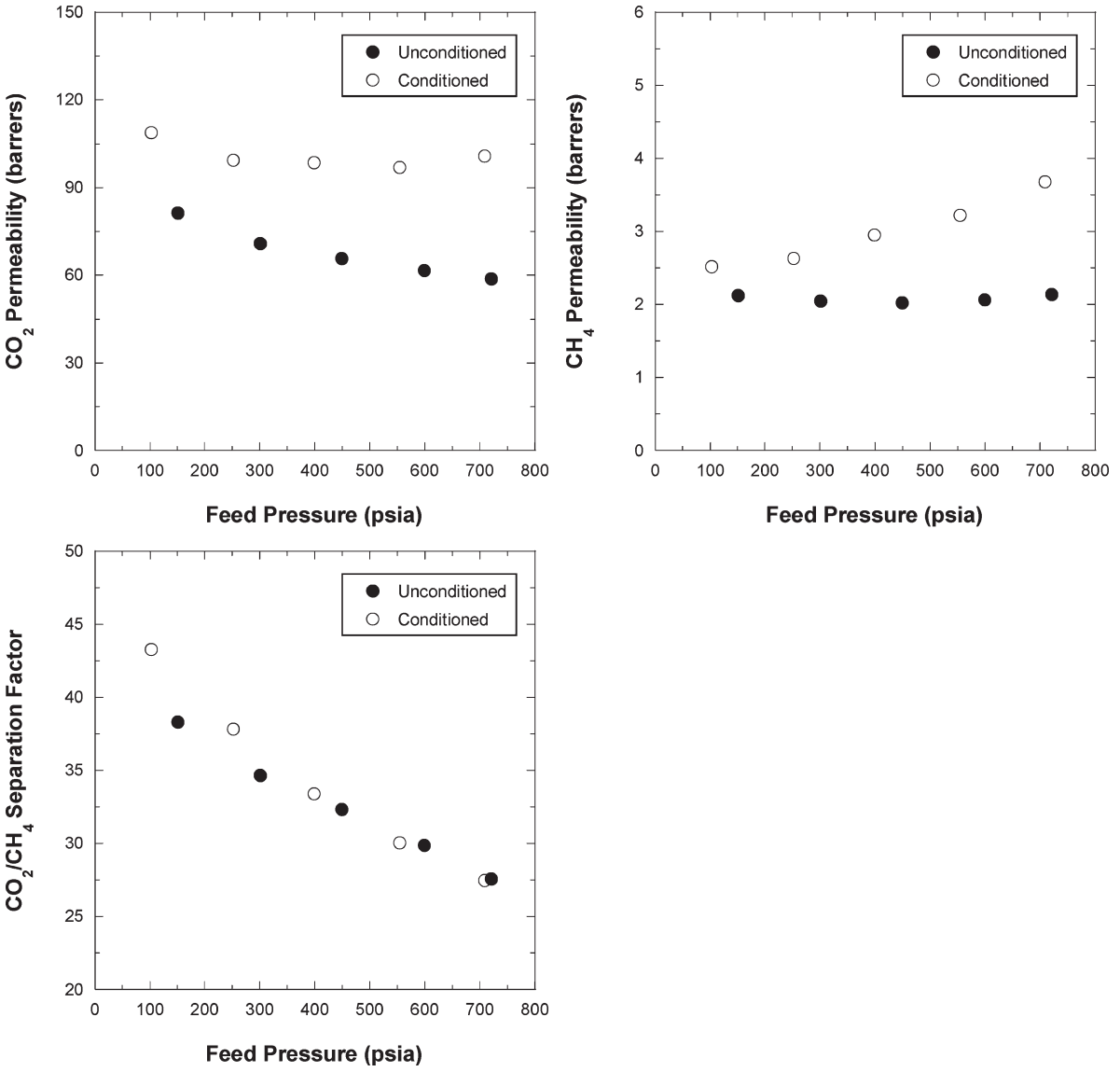

Figure 9. 50/50 CO_2/CH_4 mixed gas permeation results before and after $scCO_2$ conditioning for the ethylene glycol cross-linked polymer.

CO_2 permeability at 1500 psia following repressurization increases to match the pressurization CO_2 permeability level before the film breaks. Therefore, the ethylene glycol cross-linked film ultimately maintains its stability throughout the $scCO_2$ conditioning process for the time scale of these experiments. Conversely, the 1,4-benzenedimethanol cross-linked film has nearly identical CO_2 permeabilities at 1500 psia for both pressurization and repressurization cycles, indicating this cross-linked polymer possesses the best overall stability in the presence of $scCO_2$.

3.1.2. Mixed Gas. To probe the effects that $scCO_2$ conditioning may have on the cross-linked polymers for natural gas separations, the ethylene glycol cross-linked and 1,4-benzenedimethanol cross-linked films were examined with a 50/50 CO_2/CH_4 mixed gas feed prior to and after the $scCO_2$ conditioning in Figure 5. These results are presented in Figures 9 and 10. Both cross-linked polymers exhibit similar responses to the free acid polymer in that the CO_2 permeability remains relatively constant and the CH_4 permeability increases with increasing pressure. For comparison, the free acid CO_2 permeation and separation factor isotherms are shown in Figure 11. The free acid polymer exhibited a significant reduction in the CO_2 and CH_4 gas permeabilities following $scCO_2$ conditioning as a result of the structural reorganization that occurs during the $scCO_2$ conditioning.[15] However, the cross-linked polymer gas permeabilities generally increased compared to the unconditioned values, suggesting that additional free volume was trapped in the polymer following the $scCO_2$ conditioning cycle. This result was expected considering the typical hystereses that both cross-linked films exhibited during depressurization. Following $scCO_2$ conditioning, the ethylene glycol cross-linked polymer CO_2 permeability increases 70% at 720 psia of the 50/50 CO_2/CH_4 mixed gas feed, whereas the 1,4-benzenedimethanol cross-linked polymer CO_2 permeability only increases 35%. Surprisingly, the separation factors for both films remained relatively unchanged. Even though the additional free volume enhances the overall gas transport, the cross-linked nature of the polymer maintains the size-discriminating ability by restricting segmental mobility of the polymer.

For the purposes of natural gas purification, these monoesterified cross-linkable 6FDA-DAM:DABA (2:1) polymers are more suitable than the free acid polymer due to their greater hydrophobicity and ease of forming asymmetric hollow fibers in aqueous quench. Furthermore, the ultimately

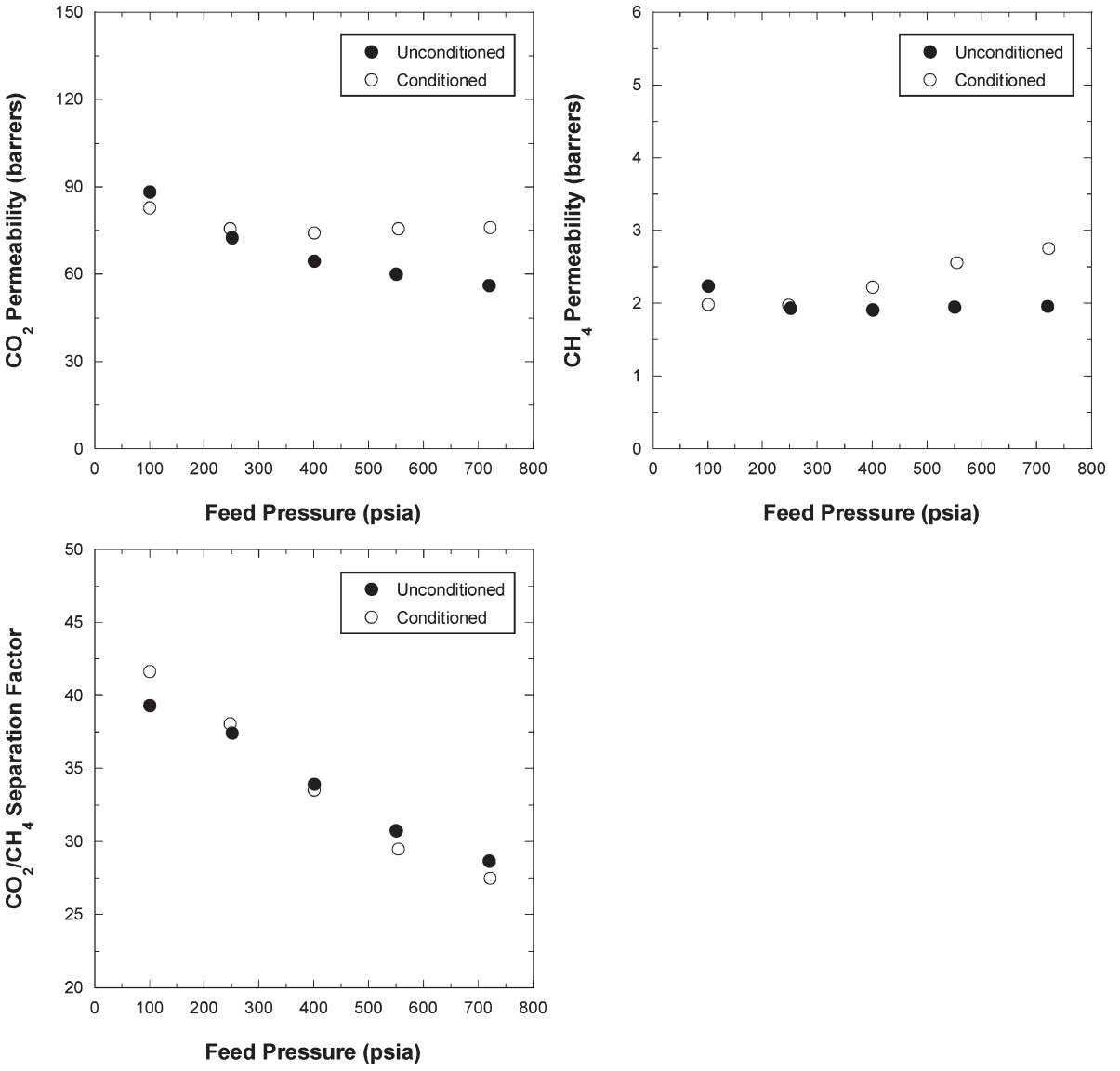

Figure 10. 50/50 CO_2/CH_4 mixed gas permeation results before and after $scCO_2$ conditioning for the 1,4-benzenedimethanol cross-linked polymer.

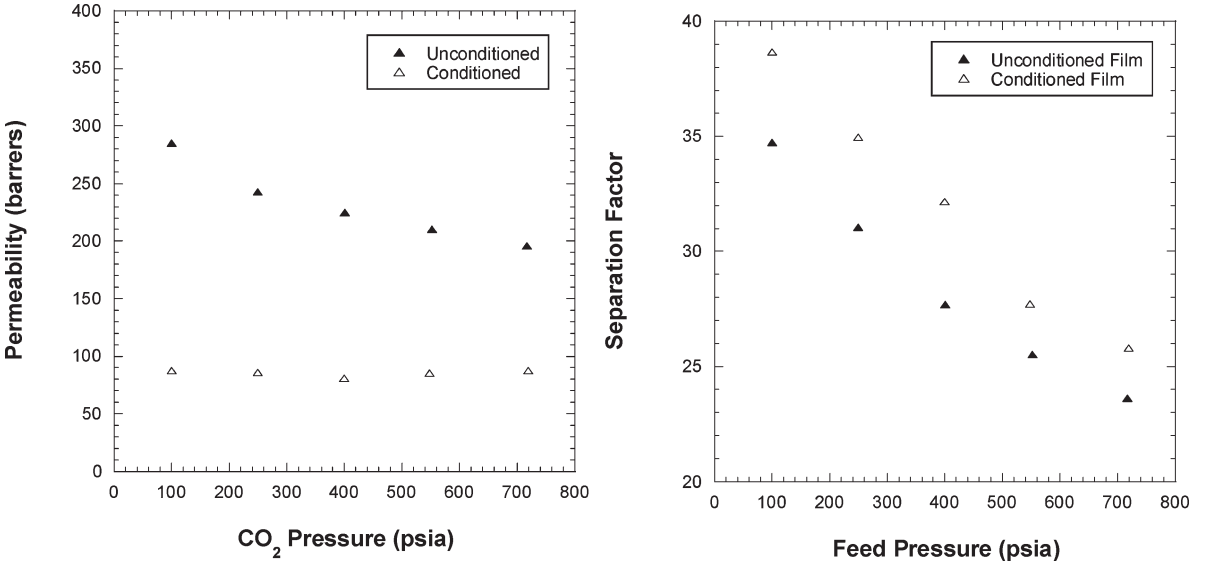

Figure 11. 50/50 CO_2/CH_4 mixed gas permeation results before and after $scCO_2$ conditioning for the free acid polymer.

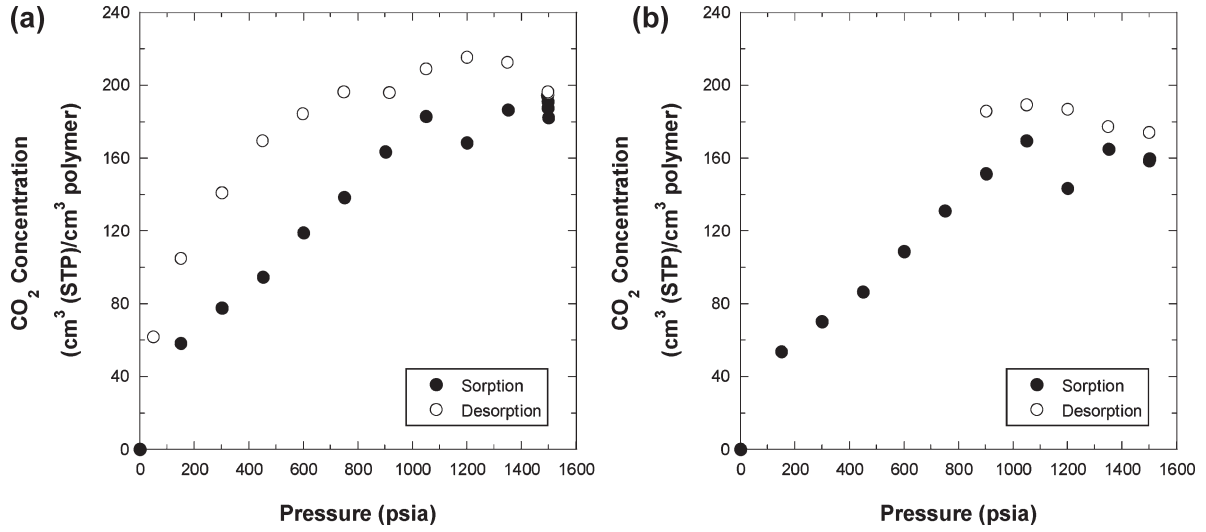

Figure 12. CO_2 sorption isotherms for the (a) ethylene glycol cross-linked and (b) 1,4-benzenedimethanol cross-linked polymers.

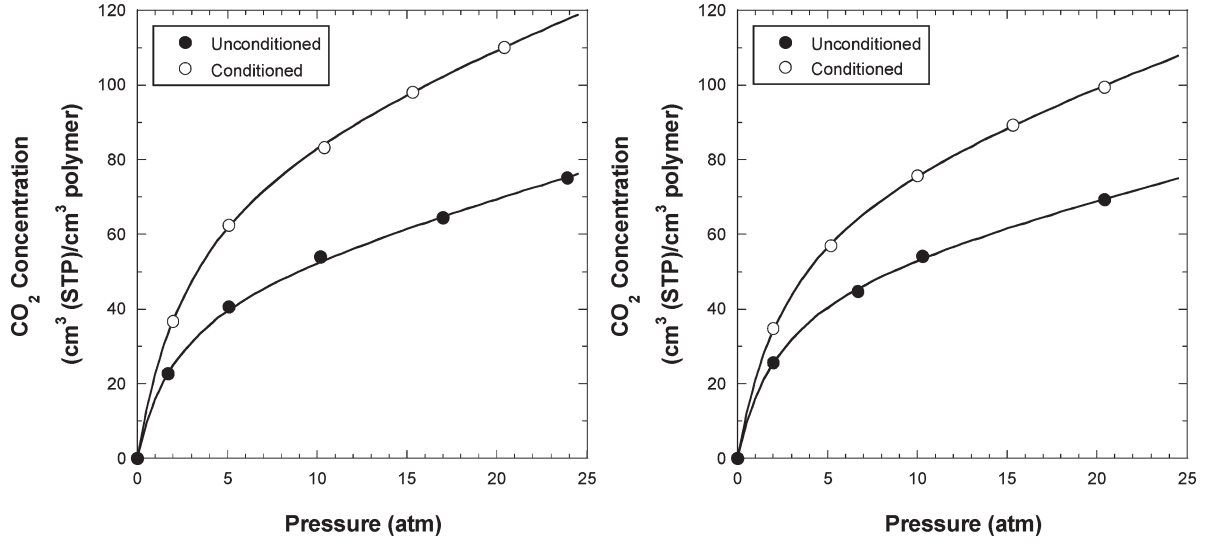

Figure 13. CO_2 sorption isotherms for the (a) ethylene glycol cross-linked and (b) 1,4-benzenedimethanol cross-linked polymers prior to and after $scCO_2$ conditioning. Lines are the dual mode model fit for each data set.

cross-linked polymers formed after thermal treatment of the monoesterified polymers are more desirable due to their increased stability in the presence of $scCO_2$ and higher gas permeabilities and selectivities following $scCO_2$ conditioning. In addition, this response reveals the possibility of tuning the separation properties of these cross-linked polymers by preconditioning the membrane with a highly soluble penetrant, like CO_2 in this case, without unnecessarily sacrificing the separation efficiency of the membrane. Between the two cross-linkable polymers, the ethylene glycol monoesterified cross-linked polymer appears to be the most feasible option since it has the highest gas throughput while maintaining the separation efficiency of the membrane.

3.2. Gas Sorption and Dilation Experiments. The $scCO_2$ conditioning sorption isotherms for the cross-linked polymers are presented in Figure 12. Both polymers exhibit the same linear response up to 1050 psia and then display a similar reduction in concentration at 1200 psia that was observed in the free acid polymer. Upon reaching 1500 psia and following 10 days of $scCO_2$ conditioning, the 1,4-benzenedimethanol cross-linked polymer has a lower sorption capacity than the ethylene glycol cross-linked polymer.

Prior to and after the above $scCO_2$ conditioning, low-pressure sorption isotherms were measured to determine the dual mode sorption parameters. The dual mode model describes gas sorption in glassy polymers through the following expression

$$C_A = k_D p_A + \frac{C'_H b}{1 + b p_A} \quad (1)$$

where C_A is the concentration of penetrant A in the polymer at a specific pressure, k_D is the Henry's law constant, C_H' is the Langmuir capacity constant, and b is the Langmuir affinity parameter. These isotherms and the corresponding model parameters are shown in Figure 13 and Table 1. These data reveal that prior to $scCO_2$ conditioning both cross-linked polymers have similar CO_2 sorption capacities; however, following $scCO_2$ conditioning, the sorption capacity of the ethylene glycol cross-linked polymer is enhanced more than the 1,4-benzenedimethanol polymer. This result is consistent with the mixed gas results for the ethylene glycol cross-linked film which exhibits a greater increase gas permeabilities following $scCO_2$ conditioning. The dual mode

Table 1. Dual Mode Model Parameters for the Cross-Linked Polymers Prior to and after $scCO_2$ Conditioning

polymer state	k_D (cm^3 STP/(cm^3 atm))	C_H' (cm^3 STP/cm^3)	b (1/atm)
ethylene glycol cross-linked pre-$scCO_2$	1.15 ± 0.07	52.5 ± 1.9	0.39 ± 0.03
ethylene glycol cross-linked post-$scCO_2$	1.81 ± 0.13	84.1 ± 3.6	0.33 ± 0.03
1,4-benzenedimethanol glycol cross-linked pre-$scCO_2$	1.15 ± 0.15	51.5 ± 3.7	0.41 ± 0.06
1,4-benzenedimethanol glycol cross-linked post-$scCO_2$	1.59 ± 0.13	77.1 ± 3.4	0.34 ± 0.03

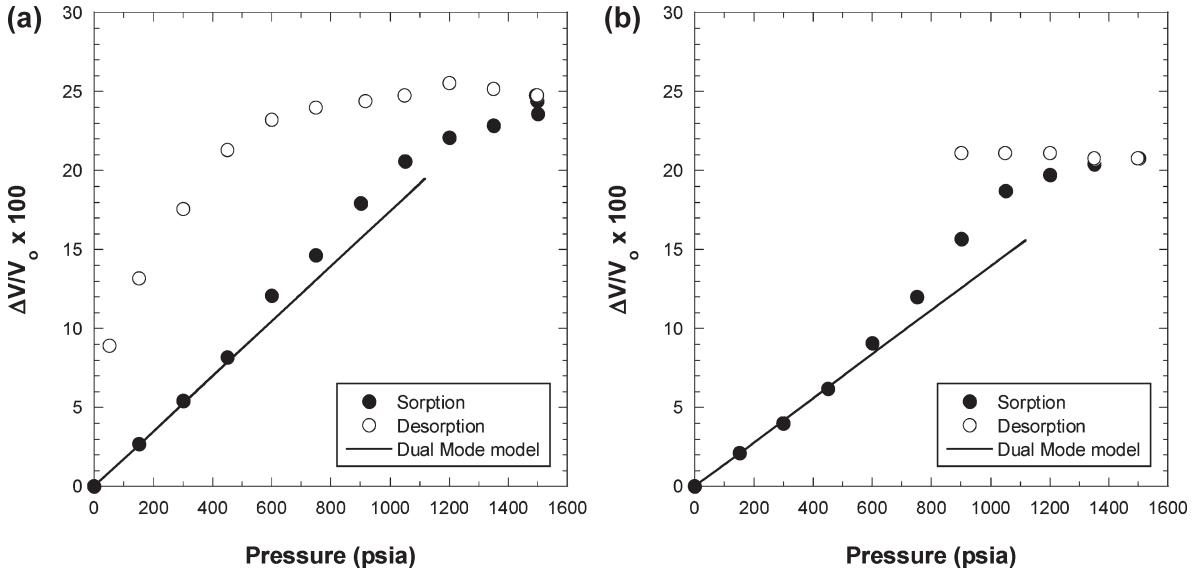

Figure 14. Dilation of the (a) ethylene glycol cross-linked and (b) 1,4-benzenedimethanol cross-linked polymers in CO_2. Lines are the dual mode model fit for dilation.

parameters confirm this sorption enhancement with a 57% and 60% increase in k_D and C_H', respectively. Conversely, the 1,4-benzenedimethanol cross-linked polymer only exhibits a 38% and 50% increase in k_D and C_H'.

Dilation measurements were taken in conjunction with the $scCO_2$ sorption measurements of the cross-linked polymers. As with the sorption isotherms, the dilation measurements indicate the 1,4-benzenemethanol cross-linked polymer is more stable with a maximum dilation of only 20%, as shown in Figure 14. Assuming polymer dilation is only a result of penetrant swelling of the Henry's law region, the dual mode model can be used to determine the partial molar volume of CO_2 in the penetrant−polymer system through the following expression

$$\frac{\Delta V}{V_0} = k_D p \frac{v_{gas}}{22415} \tag{2}$$

where v_{gas} is the partial molar volume of the penetrant in the polymer at a given pressure and the constant, 22415, is a unit conversion from cm^3 (STP) to moles. This equation, with a constant value of v_{gas}, has been used to reasonably describe a linear dilation response in polycarbonates to high CO_2 pressures.[21−23] This model is used to describe the dilation responses of the cross-linked polymers at low pressures using the preconditioned Henry's law constant. The dual mode model fits of the dilation measurements are also shown in Figure 14. The determined average partial molar volumes of CO_2 in the cross-linked polymers are 50 and 40 cm^3/mol for the ethylene glycol and 1,4-benzenedimethanol cross-linked polymers, respectively. These values are larger than the free acid polymer value of 32 cm^3/mol, indicating that the cross-linked polymers can withstand a larger percentage of the penetrant in the polymer matrix while maintaining the separating efficiency as shown in Figures 9 and 10. This lower CO_2 molar volume may reflect the higher cohesive energy density of the free acid due to hydrogen bonding between the free acid sites which makes it energetically more difficult to dilate the glassy matrix. As a point of reference, the partial molar volumes of CO_2 in substituted polycarbonates is between 42 and 48 cm^3/mol.[21] The dual mode model reasonably describes these dilation responses; however, it is evident that both cross-linked polymers deviate from the linear dual mode prediction at higher pressures through enhanced swelling. This response indicates the cross-linked polymers tend to lose their enhanced stability when conditioned at high CO_2 pressures. This response is also consistent with the enhanced permeabilities following $scCO_2$ conditioning as shown in Figures 9 and 10. However, as mentioned earlier, the separation efficiency is not greatly affected by this additional swelling.

4. Conclusions

The conditioning effects of $scCO_2$ on cross-linked 6FDA-based membranes are examined through gas permeation and sorption experiments. The responses of the cross-linked polymers are fundamentally different than that of the free acid polymer. Both the ethylene glycol and 1,4-benzenedimethanol cross-linked polymers have reduced plasticization effects which was expected; however, both cross-linked polymers also avoid the structural reorganization that was present in the free acid polymer under $scCO_2$ conditions. Fluorescence spectroscopy reveals that charge transfer complexing does not play a role in this increased stabilization for the aromatic cross-linked polymer. Because this structural reorganization does not occur in the cross-linked polymers, they exhibit a typical hysteresis upon depressurization that results in increased gas permeabilities and ultimately membrane productivity; however, as shown in the mixed gas testing, the usual consequence of a corresponding reduction in the separation factor is not observed due to the increased diffusional selectivity effects of covalent cross-linking. Therefore, this effect

highlights the possibility that the conditioning effects of a highly sorbing pentrant, like CO_2, may be used to tune the separation properties of these high-performance cross-linked polymers for specific applications. Corresponding sorption and dilation measurements of the cross-linked polymers confirm the typical hysteretical response and resulting increased sorption capacity which contributes to the enhanced permeabilities. Finally, the dual mode model reasonably describes the sorption and dilation characteristics throughout the conditioning process.

Acknowledgment. The authors acknowledge support by the United States Department of Energy (Grant DE-FG03-95ER14538) and Award KUS-I1-011-21 made by King Abdullah University of Science and Technology (KAUST) for this research.

References and Notes

(1) de Moura, J.; et al. *J. Membr. Sci.* **2007**, *299*, 138–145.
(2) Jia, D.; et al. *J. Supercrit. Fluids* **2009**, *50*, 229–234.
(3) Hamdan, S.; et al. *J. Supercrit. Fluids* **2008**, *44*, 25–30.
(4) Varona, S.; et al. *J. Supercrit. Fluids* **2008**, *45*, 181–188.
(5) Barroso, T.; et al. *J. Supercrit. Fluids* **2009**, *51*, 57–66.
(6) Ahmed, T. S.; et al. *Macromolecules* **2008**, *41*, 3086–3097.
(7) Koh, M.; et al. *Ind. Eng. Chem. Res.* **2008**, *47*, 278–283.
(8) Mazumder, S.; et al. *Transp. Porous Media* **2008**, *75*, 63–92.
(9) Shi, J. Q.; et al. *Transp. Porous Media* **2008**, *75*, 35–54.
(10) Mazzotti, M.; et al. *J. Supercrit. Fluids* **2009**, *47*, 619–627.
(11) Wallace, W. W.; et al. *Polymer* **2006**, *47*, 1207–1216.
(12) Wind, J. D.; et al. *Ind. Eng. Chem. Res.* **2002**, *41*, 6139–6148.
(13) Cao, C.; et al. *J. Membr. Sci.* **2003**, *216*, 257–268.
(14) Kosuri, M. R.; Koros, W. J. *J. Membr. Sci.* **2008**, *320*, 65–72.
(15) Kratochvil, A. K.; et al. *Macromolecules* **2009**, *42*, 5670–5675.
(16) Wind, J. D.; et al. *Macromolecules* **2003**, *36*, 1882–1888.
(17) Wind, J. D. Improving Polyimide Membrane Resistance to Carbon Dioxide Plasticization in Natural Gas Separations; University of Texas-Austin, 2002.
(18) Wachsman, E. D.; Frank, C. W. *Polymer* **1988**, *29*, 1191–1197.
(19) Kawakami, H.; et al. *J. Membr. Sci.* **1996**, *118*, 223–330.
(20) Zhou, F. B.; Koros, W. J. *Polymer* **2006**, *47*, 280–288.
(21) Fleming, G. K.; Koros, W. J. *J. Polym. Sci., Part B: Polym. Phys.* **1990**, *28*, 1137–1152.
(22) Fleming, G. K.; Koros, W. J. *Macromolecules* **1986**, *19*, 2285–2291.
(23) Fleming, G. K.; Koros, W. J. *Macromolecules* **1990**, *23*, 1353–1360.
(24) Punsalan, D. A. A Sorption and Dilation Investigation of Amorphous Glassy Polymers and Physical Aging; University of Texas-Austin, 2001.